

INCOHERENT EFFECTS DRIVEN BY THE ELECTRON CLOUD*

M. A. Furman[†] and A. A. Zholents, Center for Beam Physics, LBNL, Berkeley, CA, USA

Abstract

As a result of the synchrotron radiation from a positively-charged beam, an electron cloud is expected to develop in the vacuum chamber from the combined effects of the photoelectric and secondary emission processes [1–3]. We provide here a first estimate of the electron-cloud effect on individual particles of the beam. We focus on the space-charge tune spread, the distortion of the beta function and the dispersion, and synchro-betatron coupling. We illustrate the effects with numerical applications to the PEP-II positron ring [4]. We conclude that the magnitude of the effect is not negligible, although it is not large either. However, the present calculations can only be considered as a first estimate, since they do not include details of the electron cloud formation in different regions of the ring.

1 METHOD AND APPROXIMATIONS

We assume that an electron cloud has been established in the vacuum chamber of a positively-charged beam of closely spaced bunches. Although our analysis can be applied to any case with similar conditions, we will choose as an example the PEP-II low-energy ring (LER), which contains the positron beam.

Numerical simulations for the pumping straight chambers in the arcs of the PEP-II LER for a photon reflectivity $R \simeq 1$, photoelectric yield $Y' = 1$ and secondary electron yield corresponding to TiN, show that the electron cloud density is approximately uniform near the center of the chamber [3]. Indeed, the density on axis is $d \simeq 6.5 \times 10^5$ electrons/cm³, while its average value is $\bar{d} \simeq 4.1 \times 10^5$ electrons/cm³. For the purposes of this article we will make the approximation that the electron cloud density is uniform throughout the chamber and we will focus on the details of the electron cloud *within a positron bunch* as it traverses this uniform cloud. For vacuum chamber regions within a dipole magnetic field, the uniform-density approximation is not a good one, and a more detailed calculation is required. For the PEP-II LER, however, the pumping straight chambers account for $\sim 93\%$ of the arc length and $\sim 62\%$ of the ring circumference; hence our results, though incomplete, are meaningful.

When a bunch travels through the cloud, its head sees a density \bar{d} ; trailing positrons within the bunch sample different values of the density as the electrons are pulled in. The local electron density d is characterized by a dimensionless function $\rho(z)$ of the longitudinal coordinate z such

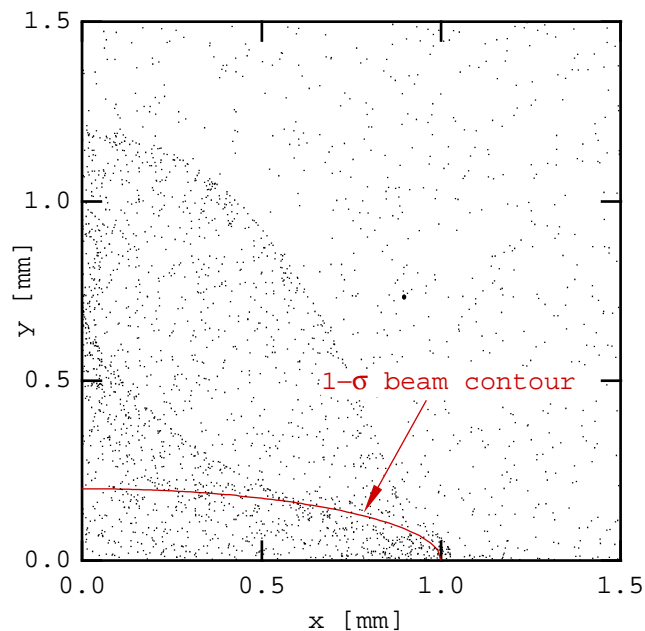


Figure 1: The electron distribution just after the bunch tail has passed. In this case, we used a sample of 100,000 static electrons initially distributed uniformly in a disk of radius 10 mm about the beam axis.

that $d = \bar{d}\rho(z)$ with $\rho(z)$ normalized such that $\rho(z) = 1$ at the head of the bunch. Making the approximation that the chamber cross-section is a perfect ellipse of semi-axes a and b , the average linear density $\bar{\lambda}$ is given, in terms of the average bulk electron density \bar{d} , by

$$\bar{\lambda} = -e\pi ab\bar{d} \quad (1)$$

while its local density is $\lambda(z) = \bar{\lambda}\rho(z)$.

In our simulations aiming at determining $\rho(z)$, we divide the bunch longitudinally into a certain number of kicks such that the “head” and “tail” kicks are located at $z = \pm z_h$. Experience shows that adequate numerical convergence is achieved with 51 equally-spaced kicks whose weight are gaussian in z with rms σ_z such that $z_h = 3\sigma_z/2$. The simulation proceeds by “injecting” a bunch into a uniform cloud of static¹ electrons, and we extract the electron density at all kick locations z . As an example, Figure 1 illustrates the transverse particle distribution just after the tail of the bunch has passed.

For the purposes of determining $\rho(z)$ we count only those electrons within the one-sigma ellipse about the bunch axis; the value of $\rho(z)$ is then the ratio of electrons

* Work supported by the US Department of Energy under contract no. DE-AC03-76SF00098. Presented at the PAC99, New York City, March 29-April 2nd, 1999.

[†] E-mail: mafurman@lbl.gov.

¹We have verified that $\rho(z)$ is not very sensitive to the initial electron-cloud average energy, up to 400 eV.

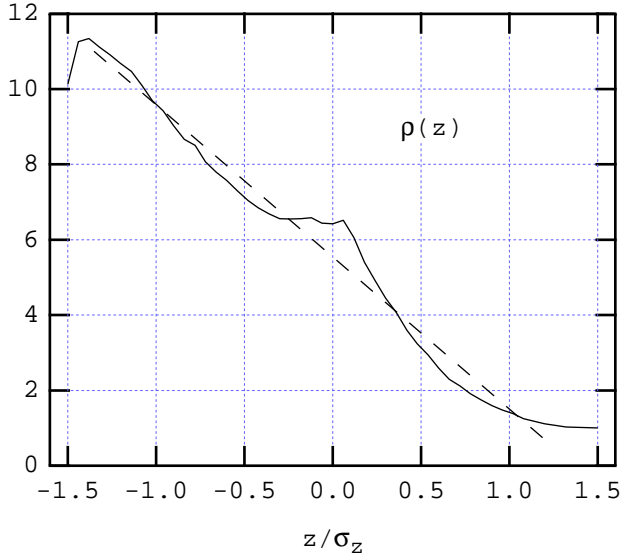


Figure 2: The electron density enhancement function $\rho(z)$ for the PEP-II LER pumping sections. The normalization is $\rho(3\sigma_z/2) = 1$. The straight line is a free-hand first-order approximation.

at kick location z relative to the number of electrons at the head of the bunch. Fig. 2 shows the result. PEP-II parameters used in the simulation are listed in Table 1.

The approximate linearity of $\rho(z)$ is a consequence of the parameter values used in the simulation. For higher values of N the electrons get pulled in more quickly into the bunch and remain temporarily trapped, leading to oscillatory behavior of $\rho(z)$. An analytic approach to this problem is described in Ref. 5.

2 TUNE SHIFT

The electric field \mathbf{E}_e from the cloud leads to a neutralization tune shift $\Delta\nu^{(n)}$ which adds to the direct space-charge tune shift $\Delta\nu^{(0)}$. A simple estimate of $\Delta\nu^{(n)}$ can be obtained by making the approximation that the transverse electron-cloud density is uniform within the bunch, as it can be qualitatively seen in Fig. 1. Our simulations show that, for nominal conditions, the kinetic energy does not exceed $\sim 8 \times 10^4$ eV, hence the electrons can be sensibly considered nonrelativistic. Thus the force on any given positron due to the electron cloud is approximately transverse and purely electric, and it is given by [6]

$$\mathbf{F}_e = e\mathbf{E}_e = \frac{4\bar{\lambda}\rho(z)}{a+b} \left(\frac{x}{a}\mathbf{i} + \frac{y}{b}\mathbf{j} \right) \quad (2)$$

where z is the longitudinal position of the positron. Inserting Eqs. 1–2 into the standard expression [7] for a tune shift yields

$$\Delta\nu_x^{(n)}(z) = \frac{r_e L \bar{\beta}_x b \bar{d}}{\gamma(a+b)} \rho(z) \quad (3)$$

where $r_e = e^2/mc^2 \simeq 2.82 \times 10^{-15}$ m is the classical electron radius, L is the aggregate length of the pumping

Table 1: Selected PEP-II parameters.

Circumference, C [m]	2200
Beam energy, E [GeV]	3.1
No. of particles per bunch, N	5.63×10^{10}
Aver. beta functions, $\bar{\beta}_x = \bar{\beta}_y$ [m]	16
Aver. hor. beam size, $\bar{\sigma}_x$ [mm]	1
Aver. ver. beam size, $\bar{\sigma}_y$ [mm]	0.2
RMS bunch length, σ_z [cm]	1
Synchrotron tune, ν_s	0.03
Chamber semi-axes, (a, b) [cm]	(4.5, 2.5)

sections, $\bar{\beta}_x$ is the average beta function and γ is the usual relativistic factor assumed $\gg 1$. A corresponding expression for $\Delta\nu_y^{(n)}$ is obtained from the above by the simultaneous substitutions $a \leftrightarrow b$ and $x \leftrightarrow y$.

Choosing the central particle ($z = 0$) as a reference, using parameter values from Table 1, setting $L = 1373$ m and $\bar{d} = 4.1 \times 10^5$ cm $^{-3}$ (obtained from separate simulations [3]) and setting $\rho(0) = 5.5$ from the linear fit in Fig. 2, we obtain

$$\left. \begin{aligned} \Delta\bar{\nu}_x^{(n)} &= 8.3 \times 10^{-3} \\ \Delta\bar{\nu}_y^{(n)} &= 1.5 \times 10^{-2} \end{aligned} \right\} \text{central particle} \quad (4)$$

for the contribution from the pumping sections. Here the bar over ν is meant to emphasize that this tune shift, which pertains to the central particle, also represents an average tune shift over the bunch, on account of the approximate linearity of $\rho(z)$.

The neutralization tune shift of the particle at the head of the bunch, which we denote with the subscript “ h ,” is obtained from Eq. (3) by setting $\rho(z_h) = 1$,

$$\left. \begin{aligned} \Delta\nu_{h,x}^{(n)} &= 1.5 \times 10^{-3} \\ \Delta\nu_{h,y}^{(n)} &= 2.7 \times 10^{-3} \end{aligned} \right\} \text{head particle} \quad (5)$$

The above expressions and numerical values should be compared with the direct space-charge tune shift of the central particle,

$$\Delta\nu_x^{(0)} = -\frac{r_e \bar{\beta}_x N C}{(2\pi)^{3/2} \gamma^3 \sigma_z \bar{\sigma}_x (\bar{\sigma}_x + \bar{\sigma}_y)} \quad (6)$$

where $\bar{\sigma}_x$ and $\bar{\sigma}_y$ are ring-averages of the rms beam sizes and N is the number of particles per bunch. A corresponding expression for $\Delta\nu_y^{(0)}$ is obtained from the above by the replacement $x \leftrightarrow y$. Substituting values from Table 1 we obtain

$$\left. \begin{aligned} \Delta\nu_x^{(0)} &= -1.3 \times 10^{-4} \\ \Delta\nu_y^{(0)} &= -6.6 \times 10^{-4} \end{aligned} \right\} \text{central particle} \quad (7)$$

3 SYNCHROBETATRON COUPLING

The z -dependence of the betatron frequency, given by

$$\omega_\beta(z) = \omega_{\beta,0} \left(1 + \Delta\nu^{(n)}(z) \right) \quad (8)$$

leads to synchrobetatron coupling. Here $\omega_{\beta,0}$ is the nominal betatron frequency, and we have neglected $\Delta\nu^{(0)}$ *vis à vis* $\Delta\nu^{(n)}$. For simplicity of the analysis we use a linear fit, $\rho(z) = \rho(0) - (\rho(0) - 1)z/z_h$. Setting $z = z_0 \sin \omega_s t$ we obtain a shifted and modulated betatron frequency, $\omega_\beta(t) = \omega'_\beta (1 - \epsilon \sin \omega_s t)$, where

$$\omega'_\beta = \omega_{\beta,0} \left(1 + \Delta\bar{\nu}^{(n)} \right) \quad (9a)$$

$$\epsilon = \frac{z_0(\rho(0) - 1)\Delta\nu_h^{(n)}}{z_h(1 + \Delta\bar{\nu}^{(n)})} \quad (9b)$$

The synchrotron angular frequency ω_s is expressed in terms of the synchrotron tune *via* $\nu_s = \omega_s/\omega_{\beta,0}$. Thus the betatron equation for the horizontal motion of a given positron is, in the smooth- β approximation,

$$\ddot{x} + \omega_\beta'^2 (1 - \epsilon \sin \omega_s t)^2 x = 0 \quad (10)$$

We have numerically integrated Eq. (10). The Fourier spectrum of $x(t)$, $\tilde{x}(\omega)$, exhibits characteristic peaks separated by $\Delta\omega = \omega_s$, as shown in Fig. 3. We assumed $\Delta\nu_h^{(n)} = 2.7 \times 10^{-3}$, $z_0/\sigma_z = 1$, and $\rho(0) = 5.5$.

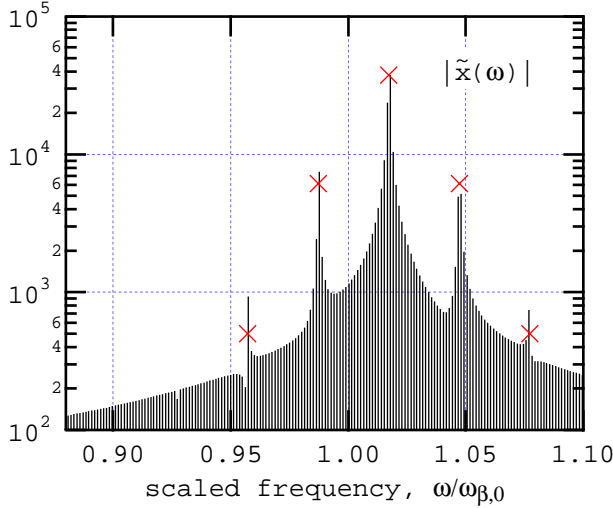


Figure 3: Unnormalized absolute-value spectrum $|\tilde{x}(\omega)|$. The frequency shift of the central peak is given by Eqs. (4)–(9a), and the sidebands are spaced by $\nu_s = 0.03$. The crosses are the values of $|J_k(\chi)|$ scaled to the main peak.

The relative height of the peaks in Fig. 3 can be understood from an approximate analytic solution [8] of Eq. (10). To order $\epsilon\omega_s/\omega'_\beta$, the spectrum is a series of delta functions at $\omega = \pm\omega'_\beta + k\omega_s$ for all integers k , with amplitude proportional to $J_k(\chi)$, where $J_k(\chi)$ is the ordinary Bessel function of order k and

$$\chi = \frac{\epsilon\omega'_\beta}{\omega_s} = \frac{z_0(\rho(0) - 1)\Delta\nu_h^{(n)}}{\nu_s z_h} = 0.32 \quad (11)$$

4 DISCUSSION

Eq. (4) represents only the contribution from the pumping sections; other regions of the ring will add to these numbers. In particular, the straight section IR2 and the wiggler section, although relatively short compared to the circumference, may develop a significant electron cloud density.

The electron cloud effectively provides a distortion of the guide field in the ring, and hence of the optics. The beta-function distortion and dispersion distortion scale as $\Delta\beta \sim \beta\Delta\nu^{(n)}/\sin 2\pi\nu$ and $\Delta\eta \sim \eta\Delta\nu^{(n)}/\sin \pi\nu$, respectively [7]. Hence these effects are small unless the tune ν is close to an integer or half-integer.

The density function $\rho(z)$, shown in Fig. 2, has higher-order components beyond the linear, as evidenced by the bump at the center. Therefore the synchrobetatron spectrum will, in general, be more complicated than what is discussed above.

When a train of bunches is injected into the ring the electron cloud has vanishing density at the head of the train and maximal density towards the tail. Therefore the tune shift $\Delta\nu^{(n)}$ will have a bunch-to-bunch variation along the train, which will introduce further complications in the synchrobetatron spectrum.

A more complete analysis describing the bunch average of the single-particle spectrum shown in Fig. 3, including the broadening effect from radiation damping, will be presented elsewhere [9].

5 ACKNOWLEDGMENTS

We are grateful to NESRC for supercomputer support.

6 REFERENCES

- [1] M. Izawa, Y. Sato and T. Toyomasu, Phys. Rev. Lett. **74**(25), 5044 (1995).
- [2] K. Ohmi, Phys. Rev. Lett. **75**(8), 1526 (1995).
- [3] M. A. Furman and G. R. Lambertson, KEK Proc. 97-17, MBI-97, Tsukuba, 15–18 July 1997, p. 170 (Y. H. Chin, ed.); <http://www.lbl.gov/~miguel/ECI-MBI97-PEPII.pdf>.
- [4] LBL-PUB-5379/SLAC-418/CALT-68-1869/UCRL-ID-114055/UC-IIRPA-93-01, June 1993.
- [5] J. S. Berg, LHC project note 97, 1 July 1997.
- [6] M. A. Furman, Am. J. Phys. **62**(12), 1134 (1994) and references therein; <http://www.lbl.gov/~miguel/ellEfield-art.pdf>.
- [7] E. D. Courant and H. S. Snyder, Ann. Phys. **3**, 1 (1958).
- [8] G. V. Stupakov and A. W. Chao, Proc. PAC95 and ICHEA, Dallas, Texas, May 1–5, 1995, p. 3288.
- [9] M. A. Furman and A. A. Zholents, to be published.